AD

TECHNICAL REPORT ARCCB-TR-95023

NONDESTRUCTIVE EVALUATION OF SPUTTERED-DEPOSITED TANTALUM CARBIDE REFRACTORY COATINGS

S.L. LEE
W.J. HEFFERNAN
J.A. WALDEN

MARCH 1995

US ARMY ARMAMENT RESEARCH,
DEVELOPMENT AND ENGINEERING CENTER
CLOSE COMBAT ARMAMENTS CENTER
BENÉT LABORATORIES
WATERVLIET, N.Y. 12189-4050

DISCLAIMER

The findings in this report are not to be construed as an official Department of the Army position unless so designated by other authorized documents.

The use of trade name(s) and/or manufacturer(s) does not constitute an official indorsement or approval.

DESTRUCTION NOTICE

For classified documents, follow the procedures in DoD 5200.22-M, Industrial Security Manual, Section II-19 or DoD 5200.1-R, Information Security Program Regulation, Chapter IX.

For unclassified, limited documents, destroy by any method that will prevent disclosure of contents or reconstruction of the document.

For unclassified, unlimited documents, destroy when the report is no longer needed. Do not return it to the originator.

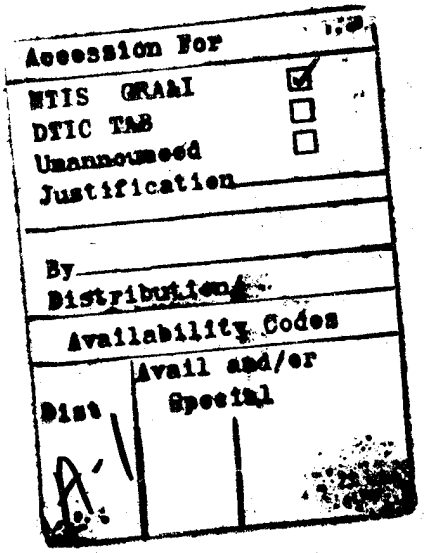

REPORT DOCUMENTATION PAGE

Form Approved
OMB No. 0704-0188

1. AGENCY USE ONLY *(Leave blank)*	2. REPORT DATE	3. REPORT TYPE AND DATES COVERED
	March 1995	Final

4. TITLE AND SUBTITLE
NONDESTRUCTIVE EVALUATION OF SPUTTER-DEPOSITED TANTALUM CARBIDE REFRACTORY COATINGS

5. FUNDING NUMBERS
AMCMS: 6111.02.H611.1

6. AUTHOR(S)
S.L. Lee, W.J. Heffernan, J. Walden

7. PERFORMING ORGANIZATION NAME(S) AND ADDRESS(ES)
U.S. Army ARDEC
Benét Laboratories, AMSTA-AR-CCB-O
Watervliet, NY 12189-4050

8. PERFORMING ORGANIZATION REPORT NUMBER
ARCCB-TR-95023

9. SPONSORING / MONITORING AGENCY NAME(S) AND ADDRESS(ES)
U.S. Army ARDEC
Close Combat Armaments Center
Picatinny Arsenal, NJ 07806-5000

10. SPONSORING / MONITORING AGENCY REPORT NUMBER

11. SUPPLEMENTARY NOTES
Presented at the Sixth International Conference on Nondestructive Characterization of Materials, Oahu, Hawaii, 7-11 July 1993. Published in the Conference Proceedings.

12a. DISTRIBUTION AVAILABILITY STATEMENT
Approved for public release; distribution unlimited

12b. DISTRIBUTION CODE

13. ABSTRACT *(Maximum 200 words)*
Desirable characteristics of refractory coatings for future projectile launchers include high wear resistance, high melting point, hardness, electrical conductivity, good adhesion, thermal stability, and high plasma resistance properties. Sputtered tantalum and tantalum compounds, such as tantalum nitride and tantalum carbide are being considered as future coatings to endure the high pressure, high temperature, and aggressive chemical environment of the bore. In this work, tantalum and tantalum carbide were reactively sputtered-deposited from argon plasmas containing methane. Nondestructive x-ray diffraction analysis determined that body-centered-cubic (*bcc*) tantalum was deposited at methane concentrations below 20 percent, face-centered-cubic (*fcc*) tantalum carbide was deposited at methane concentrations above 25 percent, and a mixture of tantalum and tantalum carbide was deposited at the transitional 22 percent methane concentration. Coating composition, crystalline structure, particle size, preferred orientations, deposition rate, Knoop hardness, and temperature coefficient of resistivity are sensitive functions of percentage methane concentration in the sputtering-deposited process.

14. SUBJECT TERMS	15. NUMBER OF PAGES
Tantalum, Tantalum Carbide, Sputtering Deposition, Refractory Coatings	21
	16. PRICE CODE

17. SECURITY CLASSIFICATION OF REPORT	18. SECURITY CLASSIFICATION OF THIS PAGE	19. SECURITY CLASSIFICATION OF ABSTRACT	20. LIMITATION OF ABSTRACT
UNCLASSIFIED	UNCLASSIFIED	UNCLASSIFIED	UL

TABLE OF CONTENTS

INTRODUCTION 1

TANTALUM CARBIDE AND TANTALUM HYDRIDE PHASE DIAGRAMS 2

X-RAY SPECTROSCOPY ANALYSIS 2

X-RAY DIFFRACTION ANALYSIS 2

DEPOSITION RATE, THERMAL COEFFICIENT OF RESISTIVITY, AND HARDNESS 5

CONCLUSIONS 7

REFERENCES 8

Tables

1. Major X-Ray Diffraction Peaks in the Tantalum Target, Sputtering Deposition Specimens Obtained at 0, 22, and 25% Methane Concentrations and Tantalum Powder and Tantalum Carbide Powder Samples 6

List of Illustrations

1. Triode sputter deposition process of tantalum and tantalum compounds 9

2. Melting point temperatures of refractory materials for bore coating applications 10

3. Diffraction patterns of sputtering deposits obtained at 0, 22, and 25 percent methane concentrations in argon plasma compared with patterns of tantalum and tantalum carbide powder specimens using a Philips diffractometer 11

4. Diffraction scan of sputtering deposit obtained at 50 percent methane and 50 percent argon concentration compared to aluminum oxide substrate and tantalum carbide powder specimen 12

5. Scintag diffractometer pattern of specimen obtained at 0 percent methane concentration as compared with scan of tantalum powder specimen and ICDD simulated diffraction pattern for tantalum 13

6. Scintag diffractometer pattern of specimen obtained at 25 percent methane concentration as compared with scan of tantalum carbide powder specimen and ICDD simulated diffraction pattern for tantalum carbide 14

7. Scintag diffractometer pattern of specimen obtained at 22 percent methane concentration as compared with simulated diffraction patterns for tantalum and tantalum carbide 15

8. Deposition rate and temperature coefficient of resistivity (TCOR) for tantalum sputtered in methane containing argon atmosphere 16

9. Change in resistivity with temperatures of tantalum/tantalum carbide coatings sputtered by variation of methane in argon 17

10. Knoop hardness for tantalum/tantalum carbide coatings sputtering in a methane-containing argon atmosphere 18

11. Deposition rate and temperature coefficient of resistivity (TCOR) of tantalum/tantalum carbide as a function of applied bias voltage 19

INTRODUCTION

Active research programs are being conducted in refractory coatings on bore surfaces by electrochemical deposition in aqueous solutions and molten salt baths and by physical vapor deposition through sputtering and evaporation processes. Objectives of the coating projects are (1) to identify and develop refractory metals, alloys, and ceramics of superior physical and chemical properties; (2) to optimize deposition process parameters to obtain strong adhesion, low stress, and uniform deposits; and (3) to characterize coating processes by nondestructive evaluation techniques. Coating the bore surfaces with refractory materials greatly improves the wear life of pressure vessel systems. In the development of electromagnetic propulsion, electrothermal propulsion, and liquid propulsion technologies, advanced bore coating materials must possess desirable thermal and electrical properties and have low reactivity to the plasma environment. As shown in Figure 1, sputtering deposition of tantalum carbide and tantalum nitride was achieved in a triode sputtering chamber, where the plasma density was controlled by adjusting the electron emission from a hot tantalum filament (ref 1).

The melting point temperatures of common refractory metals and alloys above 1000°C are given in Figure 2. Many of the metals and ceramic constituents of chromium, tantalum, molybdenum, tungsten, rhenium, etc. have been considered for advanced coating materials for future projectile launchers. Tough ceramics, such as tantalum carbide and tantalum nitride, are among the most promising. Due to the low atomic weight of carbon in heavy tantalum matrix, energy dispersive x-ray (EDX) microanalysis of specimens obtained at 0, 22, 33, and 50 percent methane concentrations in argon showed tantalum but no carbon peaks. Preliminary data on tantalum carbide sputtering deposition have been reported (refs 2,3). In this work, x-ray diffraction determined that body-centered-cubic (*bcc*) tantalum was deposited at methane concentrations below 20 percent, face-centered-cubic (*fcc*) tantalum carbide was deposited at methane concentrations above 25 percent, and a mixture of tantalum and tantalum carbide was deposited at the transitional 22 percent methane concentration. For the 22 percent methane specimen, recent wavelength dispersive x-ray fluorescence (XRF) spectrometer analysis further demonstrated both tantalum and carbon contents in the specimen. Grain size in polycrystalline materials has pronounced effects on strength and hardness; increasing strength and hardness accompanies a decrease in grain size. The introduction of methane gas in argon plasma in the sputtering chamber caused the coating deposits to transform from tantalum to tantalum carbide. Tantalum/tantalum carbide deposits consisted of very fine particle sizes. Coating composition, crystalline structure, particle size, and preferred orientations were very sensitive to methane concentrations in argon in the sputtering deposition process. As methane concentrations increase, deposition rate decreases, Knoop hardness increases, and temperature coefficient of resistivity decreases.

TANTALUM CARBIDE AND TANTALUM HYDRIDE PHASE DIAGRAMS

Binary phase diagrams of tantalum carbide and tantalum hydride were compiled by Hansen in 1958 (ref 4), Shunk in 1969 (ref 5), and Massalski in 1986 (ref 6). They disclosed phase dependence on temperature and the atomic percent of the constituents. The tantalum-carbon phase diagram discloses tantalum, tantalum carbide, and Ta_2C phases at temperatures above 1800°C, and the tantalum-hydrogen phase diagram is not well defined. Data base search for tantalum/tantalum carbide/tantalum hydride phases in the International Center for Data Diffraction (ICDD) (ref 7) results in two phases of tantalum: alpha-Ta (*bcc*), beta-Ta (*tetragonal*); two phases of tantalum carbides: TaC (*fcc*), Ta_2C (*hexagonal*), and intermediate phases with various degrees of nonstoichiometry-zeta-$TaC_{0.47}$, metastable zeta-$TaC_{0.6}$, and xi-$C_{0.71}Ta$ (*rhombohedral-hex*); several phases of tantalum hydrides: beta-TaH (*hexagonal*), Ta_2H (*orthorhombic*), and intermediate phases with various degrees of nonstoichiometry: $TaH_{0.8}$ (*orthorhombic*), $TaH_{0.9}$ (*orthorhombic*).

X-RAY SPECTROSCOPY ANALYSIS

Our EDX microanalysis of sputtered specimens was not conclusive. Spectra obtained for sputtered deposits at 0, 22, 33, and 50 percent methane concentrations in argon plasma showed tantalum peak but no carbon peak. The atomic weight of carbon is 12.01 and the atomic weight of tantalum is 180.95. It is difficult to detect low Z materials in a heavy matrix. Our Tracor XRF analyzer can chemically analyze low Z-elements only down to sodium. The coating deposit obtained at 22 percent methane concentration is of particular interest because it represents a state of co-existence of tantalum and tantalum carbide. Wavelength dispersive fluorescence spectrometer measurements were made of the 22 percent methane and 78 percent argon deposit during our recent visits to Rigaku USA (Danvers, MA) and Philips Electronics (Mahwah, NJ). Strong carbon as well as tantalum peaks were observed at both sites.

X-RAY DIFFRACTION ANALYSIS

X-ray diffraction (XRD) analysis was first performed using a semi-quantitative Philips diffractometer and then with a recently procured Scintag diffractometer. The Philips diffractometer has an LiF crystal monochromator, NaI scintillation detector, and strip-chart recorder. Molybdenum radiation was used in the study. The four-axis Scintag diffractometer has a Peltier-cooled Si(Li) detector, multi-channel spectrum analyzer, and optimized divergent receiving and scattering slits. Both molybdenum and copper radiations were used in the study.

In Figure 3, Philips diffractometer patterns of sputtering deposits obtained at 0, 22, and 25 percent methane concentrations in argon are displayed along with diffraction scans of tantalum and tantalum carbide powders obtained from Semi-Elements Inc. (Saxonburg, PA). A sieve with an opening of 0.074 mm (0.0029 inch) was used to prepare tantalum and tantalum carbide powders. The tantalum powder pattern is attributed to alpha-tantalum, and the tantalum carbide powder pattern is attributed to tantalum carbide. A comparison of the deposit pattern obtained at 0 percent methane in argon (thickness 23.24 microns on a 0.05-mm aluminum foil substrate) with the tantalum powder diffraction pattern discloses predominantly alpha-tantalum

in the sputtered sample. The pattern obtained at 22 percent methane in argon (thickness 22.73 microns on a 3-mm aluminum oxide substrate) is difficult to interpret because of the very broad and diffused diffraction peaks. The pattern indicates possible coexistence of tantalum and tantalum carbide. A comparison of the deposit pattern obtained at 25 percent methane in argon (thickness 4.8 microns on a 3-mm aluminum oxide) with the tantalum carbide powder diffraction pattern discloses a predominately tantalum carbide phase.

In Figure 4, a Philips diffraction pattern for a sputtered sample obtained at 50 percent methane and 50 percent argon (thickness 1.73 microns on 3-mm aluminum oxide substrate) is displayed along with scans for tantalum carbide powder and aluminum oxide substrate. The pattern is characterized by very broad tantalum carbide peaks superimposed on sharp diffraction peaks from the aluminum oxide substrate through tantalum carbide layers. When methane concentration in argon plasma varies from 0 to 50 percent, the deposition rate decreases from 2.5 to 0.3 microns/hour. Because of the slow deposition rate at high methane concentration, it takes a long time to obtain thicker coatings.

In Figure 5, Scintag diffraction patterns of tantalum target metal and sputtered specimen obtained at 0 percent methane are displayed along with tantalum powder scan and simulated pattern from ICDD diffraction data base. The patterns were background subtracted and K-alpha2 corrected; the simulated pattern included only K-alpha1 peak. The results are summarized as follows:

1. The randomly oriented tantalum powder has diffraction peak intensities and peak locations in agreement with the simulated tantalum pattern.

2. Tantalum target metal lines are from alpha tantalum, with major diffraction peaks shifted 0.2 degree towards lower two-theta compared to tantalum powder.

3. Full width at half maximum (fwhm) of major peaks in tantalum powder range is from 0.03 to 0.07 degrees and for two-theta from 17 to 50 degrees; tantalum target metal peaks fwhm range from 0.10 to 0.20 degrees in similar two-theta range.

4. Strong texture was observed with preferred <200>, <211>, and <411> crystalline orientations, and peak intensity diminished for the <110> orientation in the tantalum target metal.

5. The 0-degree methane deposit tantalum pattern exhibits a 0.5-degree shift towards higher two-theta, broadened lines that range from 0.3 to 0.6 degrees in the same two-theta range. The 0-degree deposit was strongly textured with <211>, <222>, <321>, and <332> preferred orientations.

In Figure 6, a Scintag diffraction pattern of sputtering deposit obtained at 25 percent methane concentration in argon is compared with diffraction scans of tantalum carbide powder and a simulated tantalum diffraction pattern. The results are summarized as follows:

1. The diffraction pattern of fine tantalum carbide powder is consistent with the pattern for tantalum carbide. Diffraction peak intensities and peak locations indicate that tantalum carbide powder was randomly oriented with peak intensities and locations identical to tantalum carbide from ICDD data base. Tantalum carbide powder lines have fwhms of 0.03 to 0.06 degrees in the range of interest.

2. The 25 percent methane deposit exhibits a 0.2 to 0.3-degree peak shift towards lower two-theta compared to the tantalum carbide pattern.

3. The fwhms for the broadened diffraction peaks range from 0.6 to 0.8 degrees and for two-theta range from 15 to 30 degrees.

4. In the 25 percent methane coating, enhanced <200> preferred crystallographic orientation was observed.

In Figure 7, a Scintag diffraction pattern of sputtering deposit obtained at 22 percent methane concentration in argon is compared to simulated tantalum and tantalum carbide diffraction data base. The very broad and diffused peaks are difficult to interpret. Coexistence of tantalum and tantalum carbide is possible, as well as other carbide and hydride phases. The two strongest lines have fwhms of 0.75 and 0.95 degrees.

Table 1 summarizes major diffraction peaks in tantalum target metal, sputtering deposition specimens obtained at 0, 22, and 25 percent methane concentrations, and tantalum and tantalum carbide powders. Diffraction line shift reflects residual stresses in the specimens, and diffraction peak broadening reflects a reduction in crystalline size by fault of certain *hkl* planes and by microstrains in the coherently diffracting domains (ref 8). In addition, carbon and hydrogen dissolution interstitially in the tantalum/tantalum carbide deposits can also cause shifts in the diffraction peaks.

In the 0 percent deposition specimen, the peak shifts to smaller d-spacings. Tensile residual stresses may be present. Alpha tantalum (*bcc*) has a lattice parameter of 3.3058 angstroms, and tantalum carbide (*fcc*) has a lattice parameter of 4.4547 angstroms. In the deposit obtained at 25 percent methane concentration, the peak shifts to larger d-spacings, which may be due to the effect of carbon dissolved in tantalum/tantalum carbide or compressive residual stresses. In addition to internal residual stresses generated in the deposition process, thermal stresses should also be considered. Furthermore, the 0 percent deposit was made on aluminum foil substrate, while the 25 percent deposit was made on aluminum oxide substrate. The shifts can be caused by the differences in thermal expansion coefficients of tantalum metal compared to the aluminum substrate and tantalum carbide ceramic compared to the aluminum oxide substrate.

For a diffraction peak around 17 degrees two-theta, the fwhm for the tantalum target was 0.16 degrees. For deposition samples at 0, 22, and 25 percent the fwhms were 0.5, 0.9, and 0.5 degrees, respectively. The fwhms for tantalum and tantalum carbide powder samples were of the order of 0.03 degrees. Deconvolution techniques using both the Scherer method (ref 9) and Warren-Averbach method (ref 10) have been applied to determine the particle size in the deposits. The methods assumed both Gaussian and Cauchy diffraction peak profiles. The results suggest that small particles sizes were generated during the deposition process, and in particular, very small particles were produced in the 22 percent transition range. Average particle sizes of approximately 55 to 100 angstroms were observed in specimens obtained at 0, 22, and 25 percent methane concentrations. According to Klug and Alexander (ref 11), when diffraction lines are very broad and diffuse, crystalline size broadening is the major cause of peak broadening. At particle sizes much less than 100 angstroms, the back-reflection lines disappear, and the low angle lines become very wide and diffuse. Average particle sizes of approximately 55 to 100 angstroms were observed in specimens obtained at 0, 22, and 25 percent methane concentrations.

DEPOSITION RATE, THERMAL COEFFICIENT OF RESISTIVITY, AND HARDNESS

Physical properties change due to changes in chemical composition and crystalline structure of the deposits. Figure 8 shows the deposition rate and temperature coefficient of resistivity (TCOR) of tantalum carbide as a function of mole fraction of methane in argon plasma. Over the range of 0 to 50 mole percent, the deposition rate varies between 2.0 and 0.3 micrometer/hour. Note especially the transition in the range of 20 to 25 mole percent methane. As the mole fraction of methane increases, TCOR varies in the range of $1.7C^{-1}*10^{3}$ to $0.0C^{-1}*10^{-3}$. Figure 9 shows the normalized resistivity of deposits of differing compositions versus temperature. It can be seen that as methane composition increases in argon plasma, the change in the resistivity decreases with temperature until the sign of the slope changes at 50 percent methane. Figure 10 shows the functional relationship between the hardness of the deposits as a function of the methane concentration. Note that the hardness increases as the mole fraction of methane increases. Figure 11 shows the dependence of deposition rate and TCOR on the bias voltage applied to the substrate. Note that the deposition rate falls off with increasing, or more negative, bias voltage, and the TCOR increases with increasing bias voltage. It is interesting to note that the deposition rate falls off with increasing bias voltage. The observation is consistent with the interpretation of an increasing sputtering effect at the substrate as the bias voltage increases. On the other hand, TCOR increases with increasing bias voltage. The observation may be rationalized by the hypothesis that the deposit is becoming more metallic, either by increasing purity of metal resulting from preferential ejection of the carbon or by the sputtering of the substrate.

Table 1. Major X-Ray Diffraction Peaks in the Tantalum Target, Sputtering Deposition Specimens Obtained at 0, 22, and 25% Methane Concentrations and Tantalum Powder and Tantalum Carbide Powder Samples

Sample Ident	Two-Theta (deg)	d-Space (angstrom)	Relative Intensity	fwhm (deg)	hkl
Ta target	24.5533	1.6679	26	0.19	Ta 200
	30.2467	1.3593	100	0.14	Ta 211
	53.9819	0.7814	25	0.10	Ta 411
	63.2812	0.6761	16	0.10	Ta 422
0% methane	17.9943	2.2678	80	0.28	Ta 110
	30.9738	1.3282	100	0.47	Ta 211
	43.9933	0.9469	92	0.53	Ta 222
	47.7592	0.8761	26	0.60	Ta 321
	60.7076	0.7018	29	0.59	Ta 332
22% methane	17.0604	2.3909	100	0.75	
	29.9441	1.3728	9	0.95	
25% methane	15.6740	2.6006	99	0.57	TaC 111
	18.1642	2.2468	100	0.59	TaC 200
	25.7890	1.5893	38	0.80	TaC 220
	30.3966	1.3528	32	0.83	TaC 311
Ta powder	17.4625	2.3363	100	0.03	Ta 110
	24.7859	1.6525	16	0.06	Ta 200
	30.4813	1.3491	35	0.05	Ta 211
	35.3300	1.1687	10	0.03	Ta 220
	39.6631	1.0454	14	0.07	Ta 310
	47.3372	0.8834	15	0.06	Ta 321
TaC powder	15.8675	2.5694	100	0.03	TaC 111
	18.4718	2.2161	73	0.08	TaC 200
	26.0900	1.5712	61	0.03	TaC 220
	30.6388	1.3424	60	0.06	TaC 311

CONCLUSIONS

In the investigation of tantalum/tantalum carbide sputtering deposition, tantalum was formed at low methane concentrations. At the threshold of 22 percent methane and 78 percent argon, there was an onset of tantalum carbide formation. As the methane concentration reached 25 percent, the coating deposit was predominately tantalum carbide. Tantalum/tantalum carbide formation was found to be a sensitive function of methane concentrations, with steep transition at 22 percent methane concentration. Summarizing our investigation of tantalum/tantalum carbide sputtering deposition, as methane concentration in argon increases from 0, 22, 25, to 50 percent, the following transitions occur in the coating deposits:

1. Crystalline structure changes from *bcc* tantalum to *fcc* tantalum carbide.

2. Diffraction peaks change from broad, to very broad and diffused, to broad.

3. Fine particle sizes of the order of 55 to 100 angstroms were observed.

4. Strong deposition residual stresses, strong preferred orientations, and effect of solid solution were observed.

5. The deposition rate decreases from 2.5 to 1 micron thickness per hour.

6. Knoop hardness increases from 820 to 1500.

7. Temperature coefficient of resistivity decreases from 1.7 to -0.1 ($C^{-1}*10^{-3}$).

The successful deposition and characterization of tantalum and tantalum carbide demonstrates a new tough ceramic for future refractory coating applications.

REFERENCES

1. S.L. Lee, W. Heffernan, and J.A. Walden, "Nondestructive Characterization of Sputtering Deposition of Tantalum and Tantalum Carbide By X-ray Diffraction," American Society for Nondestructive Testing Paper Summaries of the 1992 Spring Conference Professional Program, Orlando, FL., 1992, pp. 185-187.

2. J.A. Walden, W. Heffernan, and S.L. Lee, "Advances in Weapon Coating Technology By Physical Vapor Deposition," Research in Close Combat Weaponry, FY93 AH61 Report on Basic and Applied Research, U.S. Army Armament Research, Development, and Engineering Center, Close Combat Armaments Center, Dover, NJ, 1993, pp. 2-9 to 2-17.

3. W. Heffernan and J.A. Walden, "Sputtering Deposition of Tantalum and Tantalum Compound From Argon Plasmas Containing Methane," Research in Close Combat Weaponry, FY91 AH61 Report on Basic and Applied Research, U.S. Army Armament Research, Development, and Engineering Center, Close Combat Armaments Center, Dover, NJ, 1991, pp. 3-19 to 3-28.

4. Max Hansen, *Constitution of Binary Alloys*, McGraw-Hill Book Company, 1958, p. 380-381, p. 796-797.

5. Francis Shunk, *Constitution of Binary Alloys*, Second Edition, McGraw-Hill Book Company, 1969, p. 158, p. 409.

6. T. Massalski, *Binary Alloy Phase Diagrams*, Vols. 1 and 2, American Society for Metals, 1986, p. 592, p. 1282.

7. X-Ray Diffraction Software Data Base, International Center for Diffraction Data, Newtown Square, PA, 1994.

8. C.N.J. Wagner, M.S. Boldrick, and L. Keller, "Microstructural Characterization of Thin Polycrystalline Films By X-ray Diffraction," in: *Advances in X-Ray Analysis*, Plenum Press, 1988, pp. 129-142.

9. I.C. Noyan and J.B. Cohen, *Residual Stress Measurement and Interpretation*, Springer-Verlag, 1987.

10. B.E. Warren, *X-Ray Diffraction*, Addison Wesley, London, 1969.

11. H.P. Klug and L.E. Alexander, *X-Ray Diffraction Procedures for Polycrystalline and Amorphous Materials*, John Wiley and Sons, 1974.

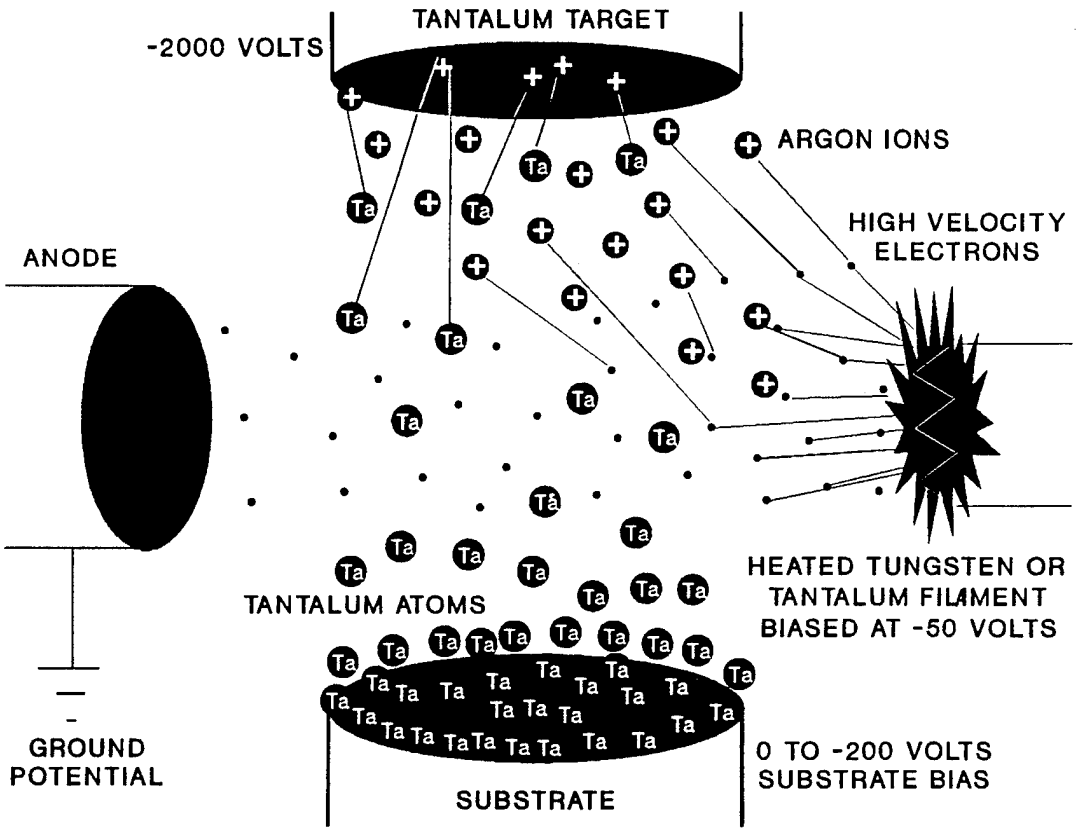

Figure 1. Triode sputter deposition process of tantalum and tantalum compounds.

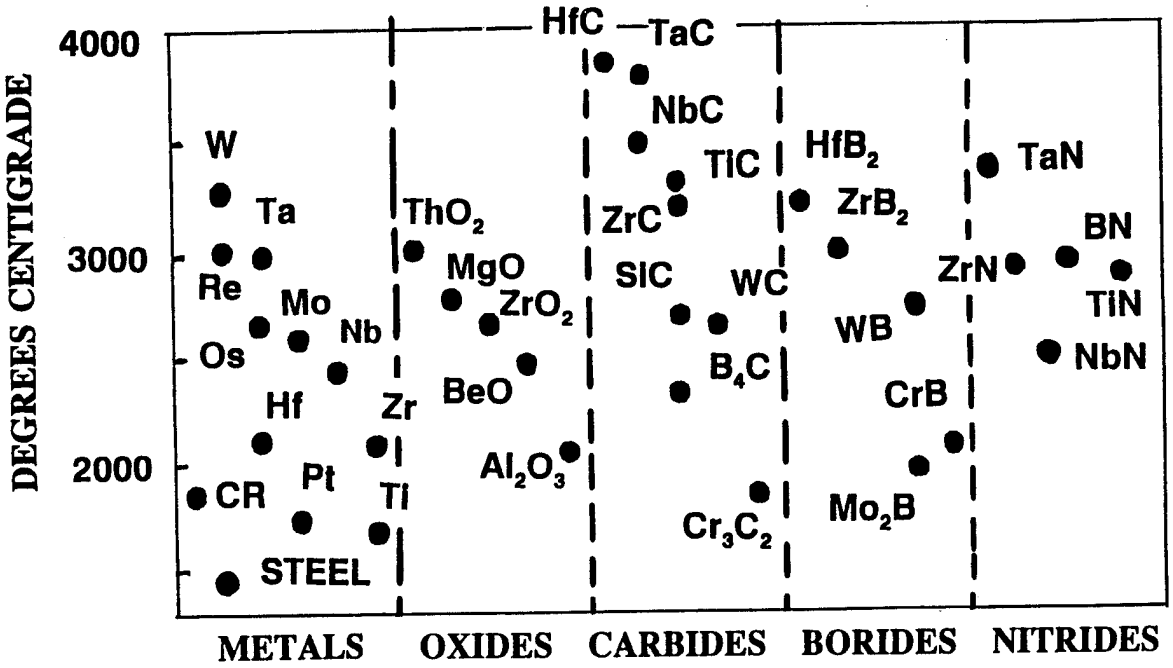

Figure 2. Melting point temperatures of refractory materials for bore coating applications.

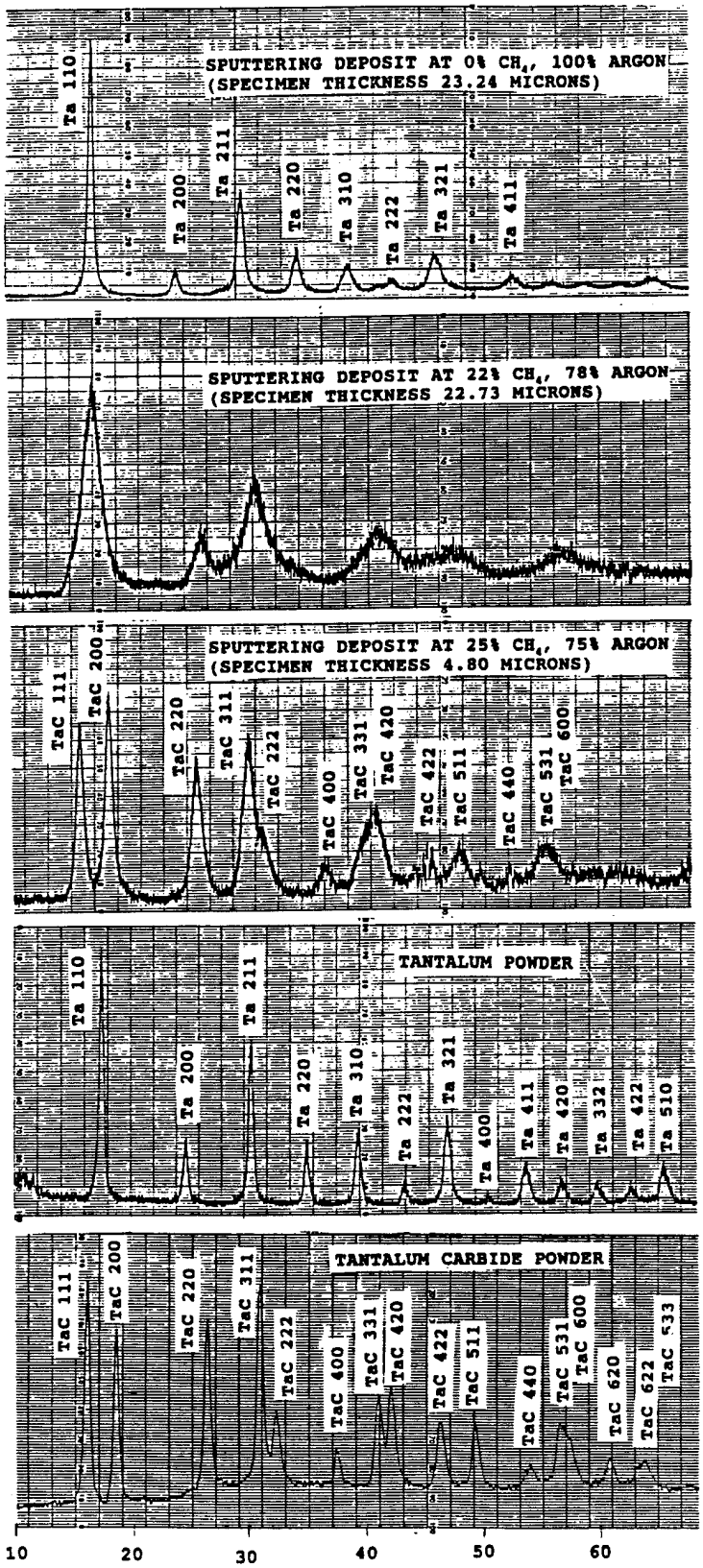

Figure 3. Diffraction patterns of sputtering deposits obtained at 0, 22, and 25 percent methane concentrations in argon plasma compared with patterns of tantalum and tantalum carbide powder specimens using a Philips diffractometer.

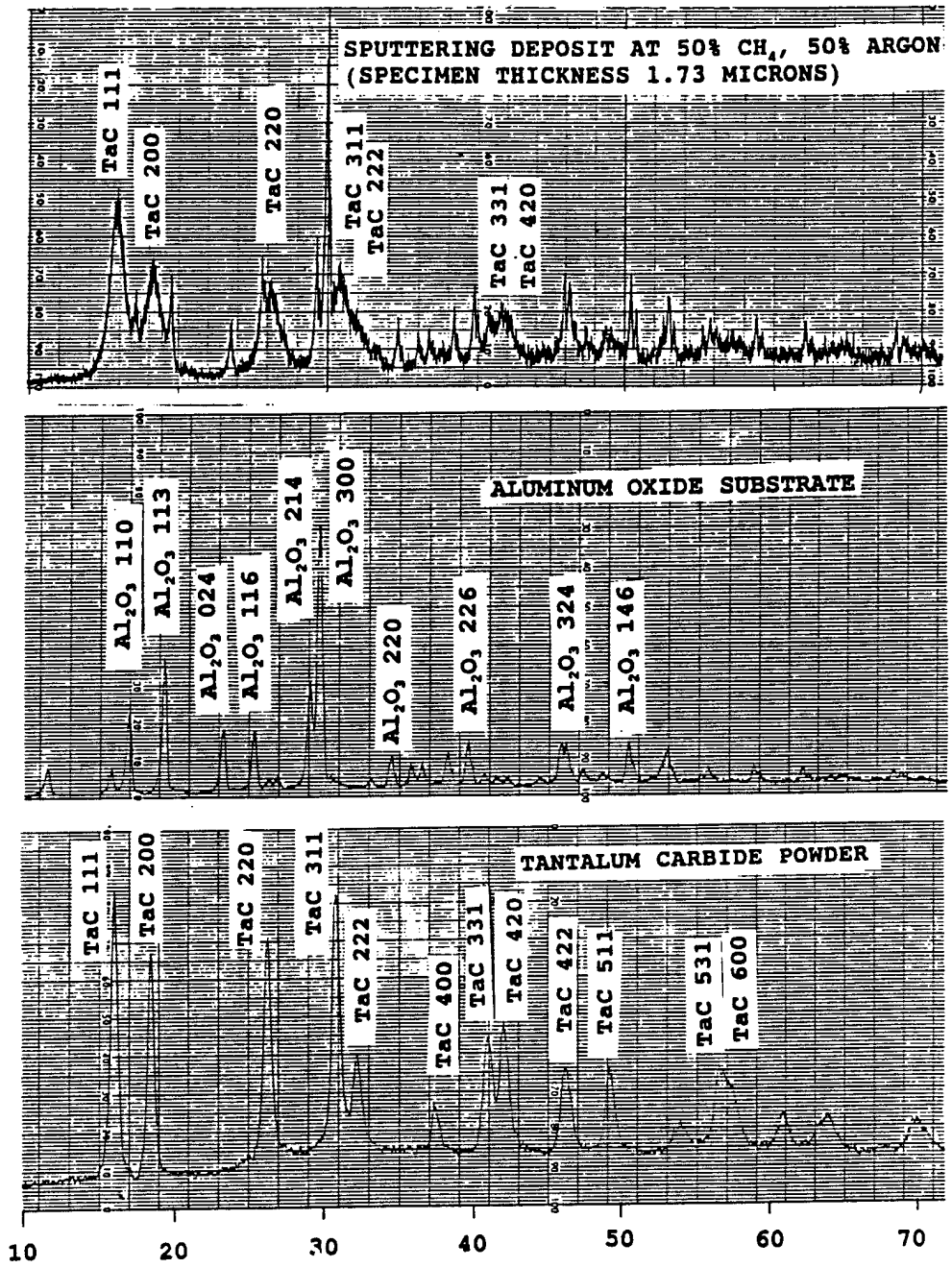

Figure 4. Diffraction scan of sputtering deposit obtained at 50 percent methane and 50 percent argon concentration compared to aluminum oxide substrate and tantalum carbide powder specimen.

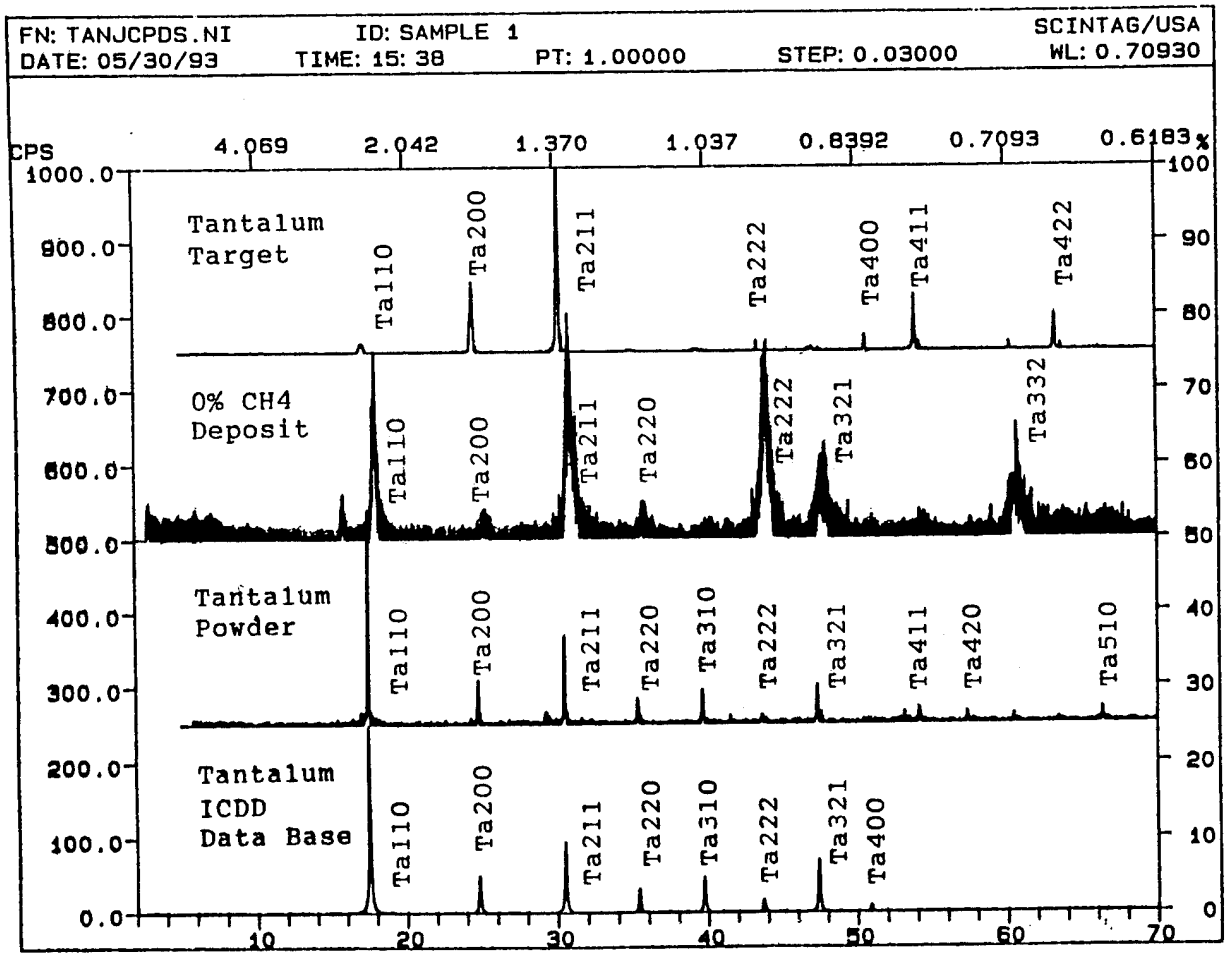

Figure 5. Scintag diffractometer pattern of specimen obtained at 0 percent methane concentration as compared with scan of tantalum powder specimen and ICDD simulated diffraction pattern for tantalum.

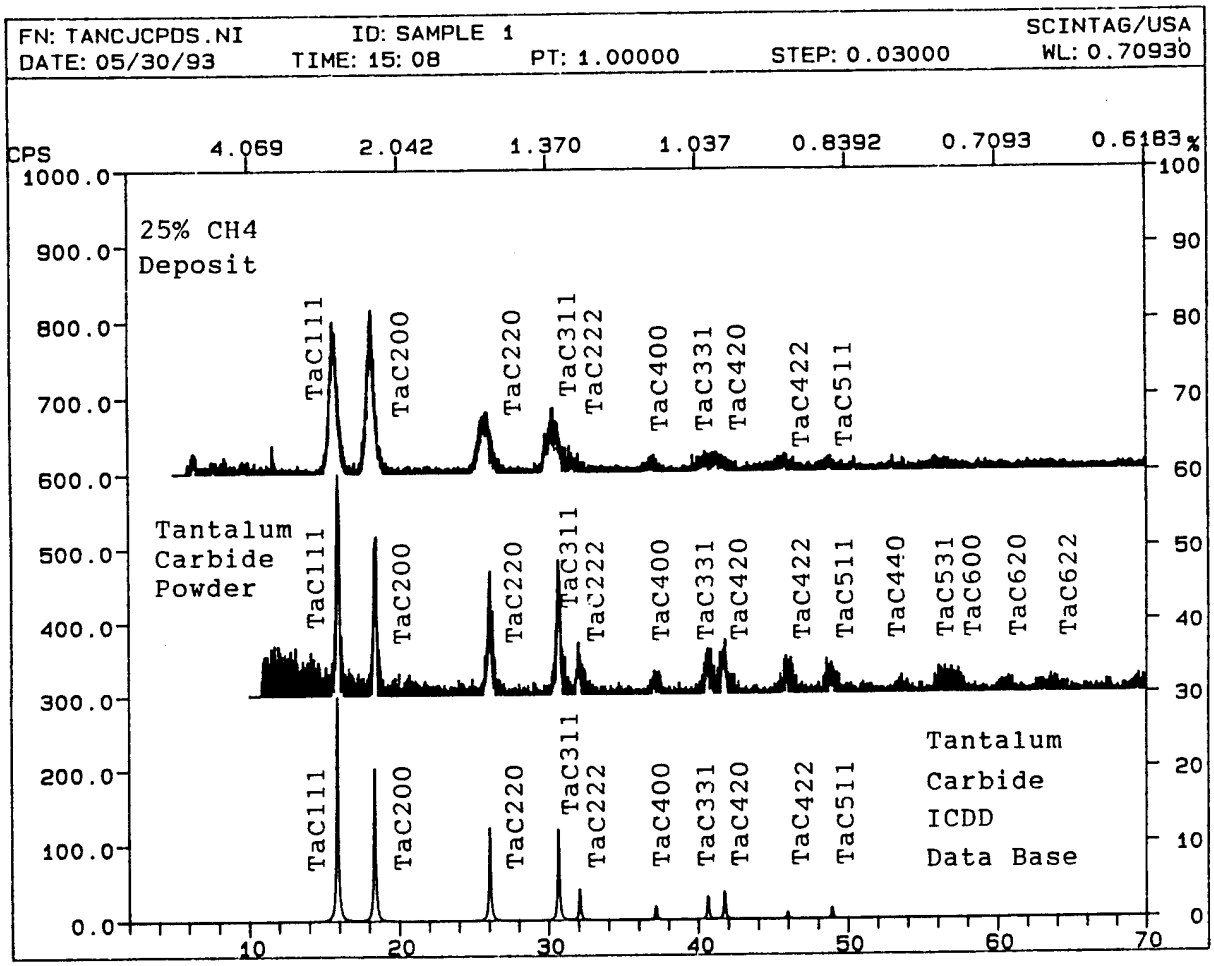

Figure 6. Scintag diffractometer pattern of specimen obtained at 25 percent methane concentration as compared with scan of tantalum carbide powder specimen and ICDD simulated diffraction pattern for tantalum carbide.

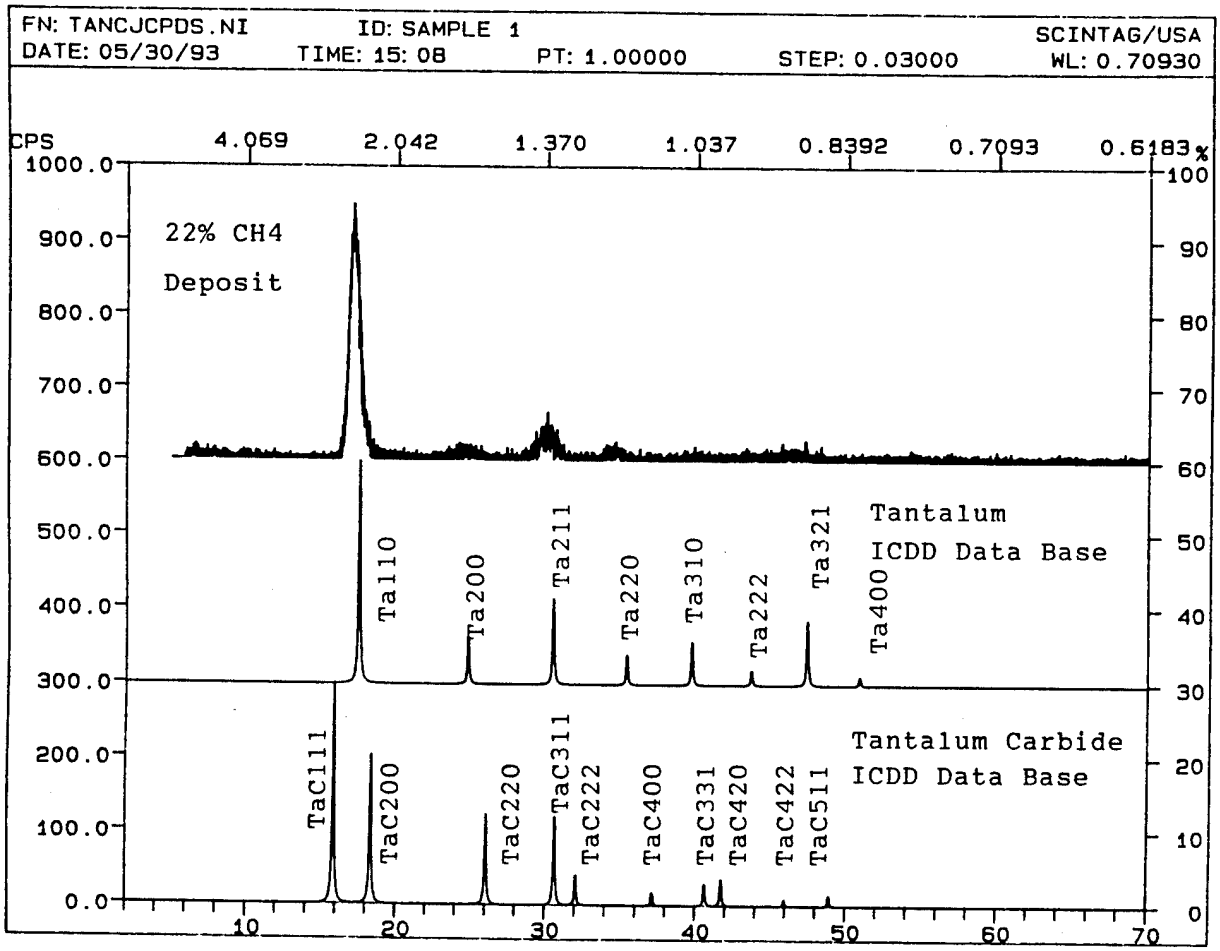

Figure 7. Scintag diffractometer pattern of specimen obtained at 22 percent methane concentration as compared with simulated diffraction patterns for tantalum and tantalum carbide.

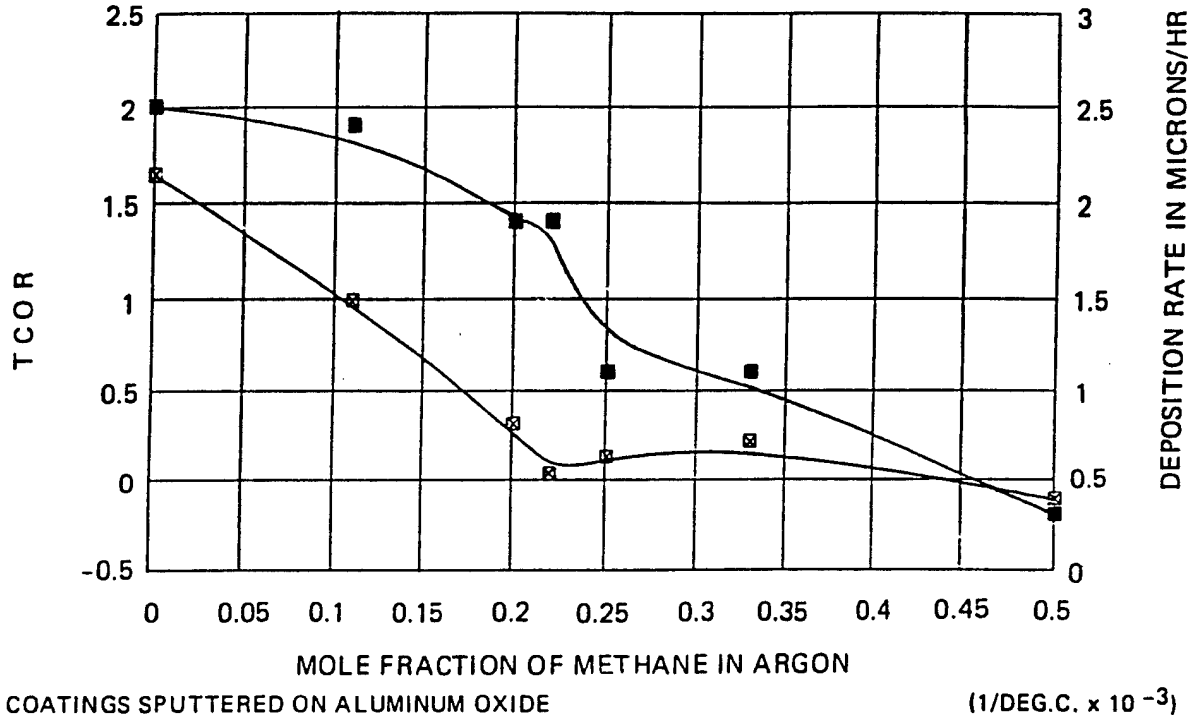

Figure 8. Deposition rate and temperature coefficient of resistivity (TCOR) for tantalum sputtered in methane containing argon atmosphere.

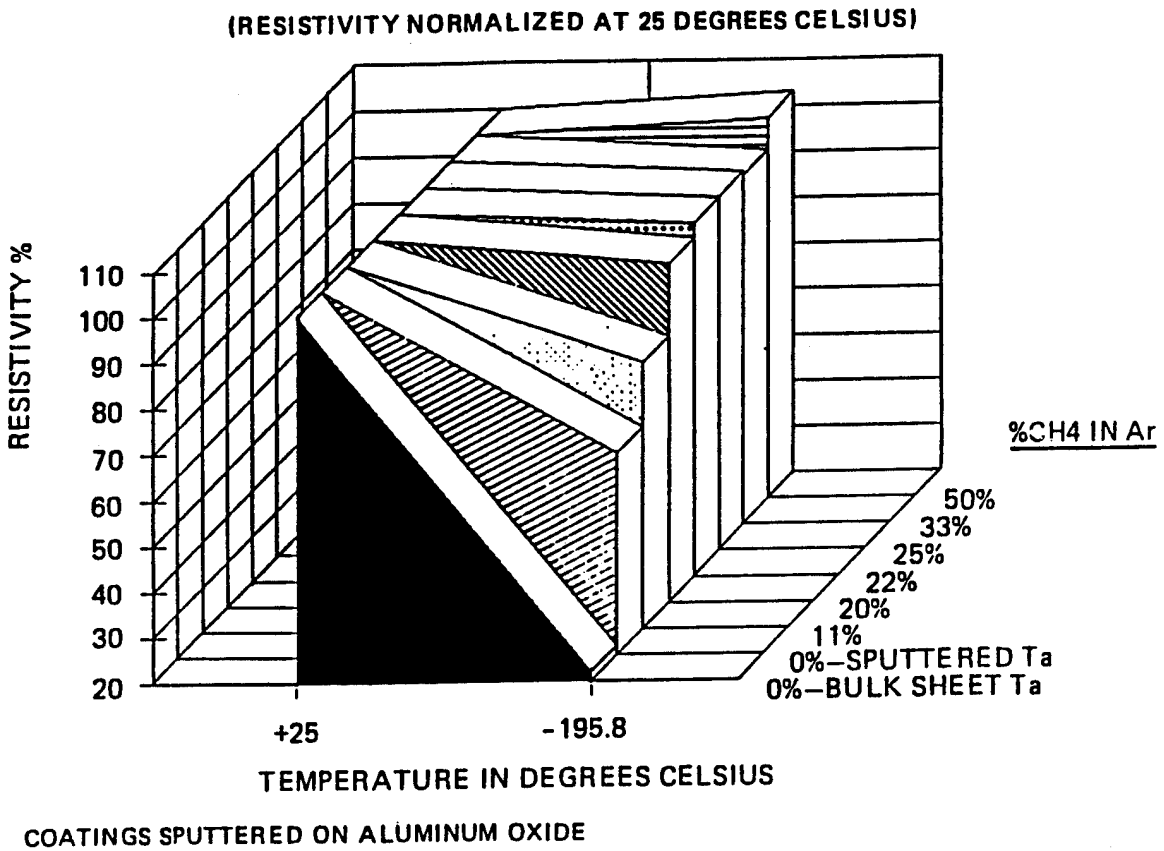

Figure 9. Change in resistivity with temperatures of tantalum/tantalum carbide coatings sputtered by variation of methane in argon.

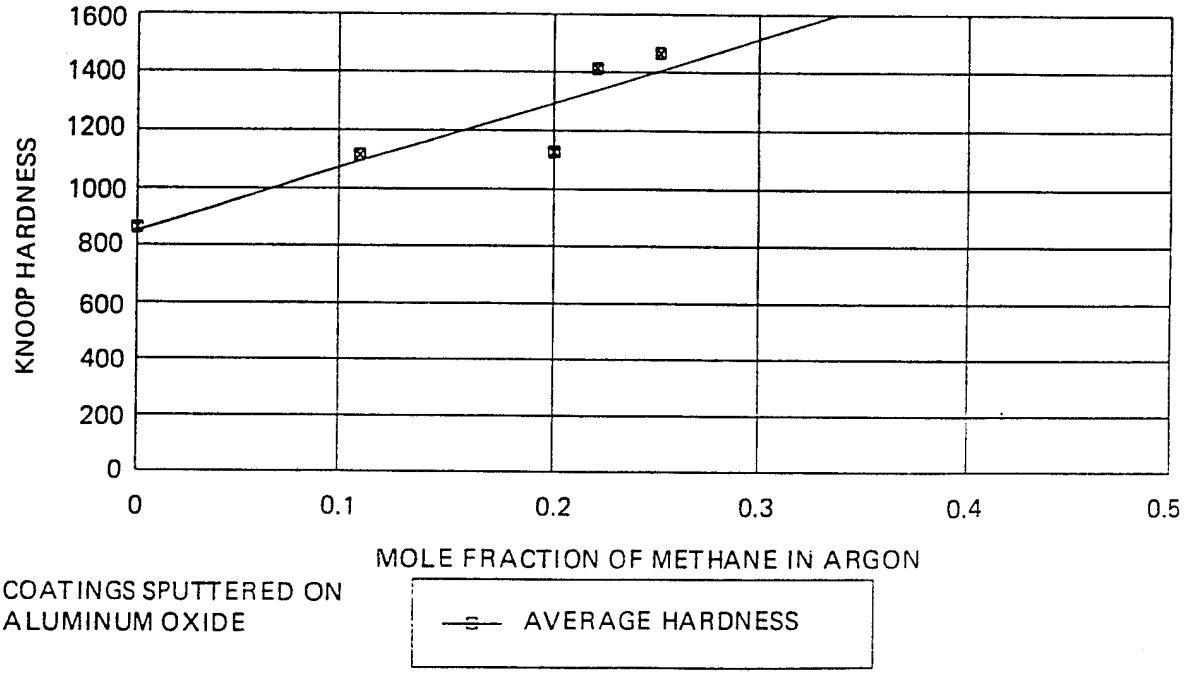

Figure 10. Knoop hardness for tantalum/tantalum carbide coatings sputtering in a methane-containing argon atmosphere.

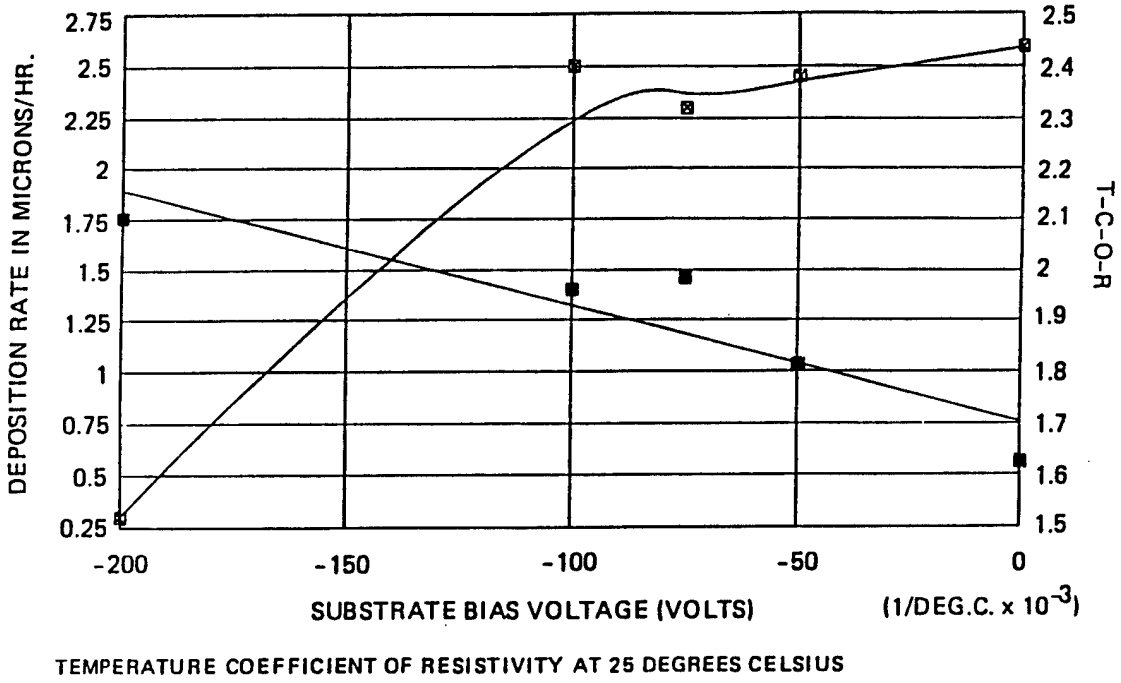

Figure 11. Deposition rate and temperature coefficient of resistivity (TCOR) of tantalum/tantalum carbide as a function of applied bias voltage.

TECHNICAL REPORT INTERNAL DISTRIBUTION LIST

	NO. OF COPIES
CHIEF, DEVELOPMENT ENGINEERING DIVISION	
ATTN: AMSTA-AR-CCB-DA	1
-DB	1
-DC	1
-DD	1
-DE	1
CHIEF, ENGINEERING DIVISION	
ATTN: AMSTA-AR-CCB-E	1
-EA	1
-EB	1
-EC	
CHIEF, TECHNOLOGY DIVISION	
ATTN: AMSTA-AR-CCB-T	2
-TA	1
-TB	1
-TC	1
TECHNICAL LIBRARY	
ATTN: AMSTA-AR-CCB-O	5
TECHNICAL PUBLICATIONS & EDITING SECTION	
ATTN: AMSTA-AR-CCB-O	3
OPERATIONS DIRECTORATE	
ATTN: SMCWV-ODP-P	1
DIRECTOR, PROCUREMENT & CONTRACTING DIRECTORATE	
ATTN: SMCWV-PP	1
DIRECTOR, PRODUCT ASSURANCE & TEST DIRECTORATE	
ATTN: SMCWV-QA	1

NOTE: PLEASE NOTIFY DIRECTOR, BENÉT LABORATORIES, ATTN: AMSTA-AR-CCB-O OF ADDRESS CHANGES.

TECHNICAL REPORT EXTERNAL DISTRIBUTION LIST

	NO. OF COPIES
ASST SEC OF THE ARMY RESEARCH AND DEVELOPMENT ATTN: DEPT FOR SCI AND TECH THE PENTAGON WASHINGTON, D.C. 20310-0103	1
ADMINISTRATOR DEFENSE TECHNICAL INFO CENTER ATTN: DTIC-OCP (ACQUISITION GROUP) BLDG. 5, CAMERON STATION ALEXANDRIA, VA 22304-6145	2
COMMANDER U.S. ARMY ARDEC ATTN: SMCAR-AEE	1
SMCAR-AES, BLDG. 321	1
SMCAR-AET-O, BLDG. 351N	1
SMCAR-FSA	1
SMCAR-FSM-E	1
SMCAR-FSS-D, BLDG. 94	1
SMCAR-IMI-I, (STINFO) BLDG. 59 PICATINNY ARSENAL, NJ 07806-5000	2
DIRECTOR U.S. ARMY RESEARCH LABORATORY ATTN: AMSRL-DD-T, BLDG. 305 ABERDEEN PROVING GROUND, MD 21005-5066	1
DIRECTOR U.S. ARMY RESEARCH LABORATORY ATTN: AMSRL-WT-PD (DR. B. BURNS) ABERDEEN PROVING GROUND, MD 21005-5066	1
DIRECTOR U.S. MATERIEL SYSTEMS ANALYSIS ACTV ATTN: AMXSY-MP ABERDEEN PROVING GROUND, MD 21005-5071	1
COMMANDER ROCK ISLAND ARSENAL ATTN: SMCRI-ENM ROCK ISLAND, IL 61299-5000	1
MIAC/CINDAS PURDUE UNIVERSITY P.O. BOX 2634 WEST LAFAYETTE, IN 47906	1
COMMANDER U.S. ARMY TANK-AUTMV R&D COMMAND ATTN: AMSTA-DDL (TECH LIBRARY) WARREN, MI 48397-5000	1
COMMANDER U.S. MILITARY ACADEMY ATTN: DEPARTMENT OF MECHANICS WEST POINT, NY 10966-1792	1
U.S. ARMY MISSILE COMMAND REDSTONE SCIENTIFIC INFO CENTER ATTN: DOCUMENTS SECTION, BLDG. 4484 REDSTONE ARSENAL, AL 35898-5241	2
COMMANDER U.S. ARMY FOREIGN SCI & TECH CENTER ATTN: DRXST-SD 220 7TH STREET, N.E. CHARLOTTESVILLE, VA 22901	1
COMMANDER U.S. ARMY LABCOM MATERIALS TECHNOLOGY LABORATORY ATTN: SLCMT-IML (TECH LIBRARY) WATERTOWN, MA 02172-0001	2
COMMANDER U.S. ARMY LABCOM, ISA ATTN: SLCIS-IM-TL 2800 POWER MILL ROAD ADELPHI, MD 20783-1145	1

NOTE: PLEASE NOTIFY COMMANDER, ARMAMENT RESEARCH, DEVELOPMENT, AND ENGINEERING CENTER, BENÉT LABORATORIES, CCAC, U.S. ARMY TANK-AUTOMOTIVE AND ARMAMENTS COMMAND, AMSTA-AR-CCB-O, WATERVLIET, NY 12189-4050 OF ADDRESS CHANGES.

TECHNICAL REPORT EXTERNAL DISTRIBUTION LIST (CONT'D)

	NO. OF COPIES
COMMANDER U.S. ARMY RESEARCH OFFICE ATTN: CHIEF, IPO P.O. BOX 12211 RESEARCH TRIANGLE PARK, NC 27709-2211	1
DIRECTOR U.S. NAVAL RESEARCH LABORATORY ATTN: MATERIALS SCI & TECH DIV CODE 26-27 (DOC LIBRARY) WASHINGTON, D.C. 20375	1 1
WRIGHT LABORATORY ARMAMENT DIRECTORATE ATTN: WL/MNM EGLIN AFB, FL 32542-6810	1
WRIGHT LABORATORY ARMAMENT DIRECTORATE ATTN: WL/MNMF EGLIN AFB, FL 32542-6810	1

NOTE: PLEASE NOTIFY COMMANDER, ARMAMENT RESEARCH, DEVELOPMENT, AND ENGINEERING CENTER, BENÉT LABORATORIES, CCAC, U.S. ARMY TANK-AUTOMOTIVE AND ARMAMENTS COMMAND, AMSTA-AR-CCB-O, WATERVLIET, NY 12189-4050 OF ADDRESS CHANGES.